

1 Scale-similarity model for Lagrangian velocity correlations in isotropic and stationary turbulenceGuo-Wei He,^{*} Guodong Jin, and Xin Zhao*LNM, Institute of Mechanics, Chinese Academy of Sciences, Beijing 100080, People's Republic of China*

(Received 4 May 2009)

A scale-similarity model for Lagrangian two-point, two-time velocity correlations (LVCs) in isotropic turbulence is developed from the Kolmogorov similarity hypothesis. It is a second approximation to the isocontours of LVCs, while the Smith-Hay model is only a first approximation. This model expresses the LVC by its space correlation and a dispersion velocity. We derive the analytical expression for the dispersion velocity from the Navier-Stokes equations using the quasinormality assumption. The dispersion velocity is dependent on enstrophy spectra and shown to be smaller than the sweeping velocity for the Eulerian velocity correlation. Therefore, the Lagrangian decorrelation process is slower than the Eulerian decorrelation process. The data from direct numerical simulation of isotropic turbulence support the scale-similarity model: the LVCs for different space separations collapse into a universal form when plotted against the separation axis defined by the model.

DOI: XXXX

PACS number(s): 47.27.Ak, 05.45.-a

I. INTRODUCTION

The turbulent diffusion process is naturally described by the relative separations of particle pairs in Lagrangian coordinates [1–3]. Following Taylor's pioneering work [4], Batchelor expressed the root-mean-square of the relative separations by the integration of Lagrangian velocity correlation (LVC) [5,6]. Therefore, an accurate prediction on relative dispersions is essentially dependent on LVC modeling. In the probability density function (PDF) approach [7–9] and various turbulence closure theories [2,10], the LVC provides a relaxation time scale as an input to close the transport equations. A related question is the relationship between Lagrangian and Eulerian velocity correlations [11–13], which yields the different predictions on the scaling of energy spectra. The recent application of large-eddy simulation (LES) to particle-laden turbulence raises such a question as whether or not LES could correctly predict LVCs [14]. The existing subgrid scale models (SGS) are mostly constructed to predict the spatial statistics such as energy spectra [15,16]. However, these models may not accurately predict LVCs since the LVCs are not dependent on energy spectra alone. A LVC model is helpful to develop a SGS model for LES of particle-laden turbulence. In this paper, we will develop a scale-similarity model for Lagrangian velocity correlations. The inherent difficulty in developing a LVC model is that a LVC depends on its instantaneous space separations. Therefore, the LVC and the relative separation are strongly correlated and thus their relationship forms an unclosed equation. This implies that the possession of such a relationship would be equivalent to solve a turbulence closure problem. Starting with the Taylor frozen flow hypothesis, Smith and Hay [17] developed a model which expresses the LVC by an Eulerian velocity correlation and a linear transformation of space and time separations. We will show in next section that this model is a first approximation to the isocor-

relation contours. Some corrections [18] to the Smith-Hay model were made to include the nonfrozen flow effect with some successes. The critical assumption in those corrections is that the LVCs have the same shape as the Eulerian velocity correlations with different decorrelation time scales. Taylor assumed that the space and time variables in the LVC are separable [6]. This implies that the LVC is a simple product of Eulerian velocity correlations and one-point LVC. This assumption suppresses the space-scale-dependence of the temporal part of LVCs.

Since both Lagrangian and Eulerian velocity correlations are determined by the same turbulent flows, there must exist a relationship between those two quantities. To understand this issue, we define a two-point and two-time Lagrangian velocity correlation or simply Lagrangian velocity correlation as follows:

$$R(r, \tau) = \langle \mathbf{v}(\mathbf{x}_0 + \mathbf{r}, t_0 | t_0 + \tau) \cdot \mathbf{v}(\mathbf{x}_0, t_0 | t_0) \rangle, \quad (1)$$

where $\mathbf{v}(\mathbf{x}, t_0 | t_0 + \tau)$ is the velocity, measured at time $t_0 + \tau$, of the fluid particle that passes through the point \mathbf{x} at time t_0 . τ is a time separation which is either positive for a forward trace or negative for a backward trace. \mathbf{r} denotes a space separation vector with its magnitude $r = |\mathbf{r}|$ and $-\mathbf{r}$ denotes the space separation vector of the separation $-r = -|\mathbf{r}|$. The bracket $\langle \cdots \rangle$ denotes the ensemble average. The correlation function is independent of the spatial location \mathbf{x}_0 and the starting time t_0 due to the homogeneity and stationarity. When $r=0$, the LVC $R(r, \tau) = R(0, \tau)$ is the Lagrangian one-point, two-time correlation. When $\tau=0$, the LVC $R(r, \tau) = R(r, 0)$ coincides with the conventional two-point Eulerian velocity correlation. Kolmogorov's similarity hypothesis [19] yields a self-similar function for either space correlation $R(r, 0)$ or time correlation $R(0, \tau)$. However, the space-time correlation function $R(r, \tau)$ remains unknown [20].

To pursue this relationship, the two-point, one-time LVC is expressed in terms of the joint PDF of the relative separation and Eulerian velocity. Corrsin [21] proposed the well-known independent hypothesis that the PDF of relative separations are independent of that of the Eulerian velocity fields. The hypothesis circumvents the main difficulty in relating

^{*}Author to whom all correspondence should be addressed; hgw@lnm.imech.ac.cn; guoweihe@yahoo.com

Lagrangian velocity correlations with Eulerian ones and yields an approximate relationship between the Lagrangian and Eulerian velocity correlations. Latter on, this result is shown to be equivalent to the first-order truncation of renormalized perturbation expansion [22]. Among the statistic theories of turbulence, direct interaction approximation (DIA) [23] and Lagrangian renormalization approximation (LRA) [24] are typically used to calculate the LVCs. They successfully predict the scaling of LVCs in the inertial sub-range with good agreements with the DNS results. However, no explicit model can be analytically deduced from either of the DIA and LRA equations. Gotoh and Kaneda [25] used the Taylor series expansion to calculate the Lagrangian time scales. The short-time analysis also yields a good prediction on the scaling of Lagrangian time scales. The Langevin equations can be also used to calculate LVCs [2,26–28]. Recent experimental measurements [29] on pair dispersion in turbulent flows attract the attention to Lagrangian statistics and raise such a problem of the intermittency correction to Lagrangian time scales.

In this paper, we will develop a scale-similarity model for LVC using the isocorrelation contours, which is related to the Eulerian velocity correlation with an additional parameter. The isocorrelation contours represent a similarity transformation which links the properties of the LVC at different scales in space and time. Once the transformation is applied to link the two-point, two-time LVCs with the two-point, one-time LVCs, it yields a scale-similarity model.

The organization of this paper is as follows: we will derive the scale-similarity model in Sec. II. Unlike the Smith-Hay model, the present model doesn't depend on the Taylor frozen flow hypothesis. It is a second approximation to the isocorrelation contours while the Smith-Hay model is only a first approximation. Using the Kolmogorov similarity hypothesis, this model can be generalized to the space and time separations in the inertial range. It shares the short-time behaviors with the results from Taylor series expansions, but it is valid for larger separations in both space and time. We analytically derive the expression for the dispersion velocity, which is the only one parameter in the scale-similarity model in Sec. III. This derivation is based on the conventional quasnormality assumption. From the expression of the dispersion velocity, we confirm the intuitive prediction that the Lagrangian decorrelation time scale is larger than the Eulerian one. The direct numerical simulation (DNS) of isotropic turbulence will be used to verify the scale-similarity model in Sec. IV. The data from DNS supports the scale-similarity model in the sense of that the correlation curves collapse together when they are rescaled using the present model. Finally, the discussion and conclusions are made in Sec. V.

II. SCALE-SIMILARITY MODEL

AQ: In this section, we will first present the scale-similarity model for Lagrangian velocity correlations and then present its derivation. The scale-similarity model expresses a two-point and two-time LVC $R(r, \tau)$ by the Eulerian velocity correlation $R(r, 0)$ and a parameter V , namely,

$$R(r, \tau) = R(\sqrt{r^2 + V^2 \tau^2}, 0). \quad (2)$$

Here, V is a dispersion velocity which will be explained later. The model incorporates the time separation into the argument of the space separation in the Eulerian velocity correlations. The well-known Smith-Hay model suggests

$$R(r, \tau) = R(r + U\tau/\beta, 0), \quad (3)$$

where U is a sweeping velocity defined as root-mean-square of fluctuation velocities and β a constant ratio of Lagrangian to Eulerian integral time scales. The Smith-Hay model and its variations imply that the isocorrelation contours are straight lines. This implication violates the property of correlation functions which should decay as either space or time separation increases negatively. The scale-similarity model does exhibit this property.

The present model is based on the scale-similarity behavior of the LVCs, which is the consequence of the Kolmogorov similarity hypothesis. Figure 2 shows the isocorrelation contours from the DNS data of isotropic turbulence, whose details will be given in Sec. IV. It is clearly seen that they are closed curves of maximal chord length in the space separation axis and minimal chord length in the time separation axis. The overall shapes of the isocorrelation contours are mainly determined by the aspect ratio that is the ratio of the maximal chord length to the minimal chord one. An empirical observation suggests that the isocorrelation contours are self-similar in the sense of that their aspect ratios satisfy a power law. This can be justified from the classic Kolmogorov similarity hypothesis as follows: we introduce the second-order Lagrangian velocity structure function in both space and time

$$D(r, \tau) = \langle [v_i(\mathbf{x} + \mathbf{r}, t|t + \tau) - v_i(\mathbf{x}, t|t)]^2 \rangle. \quad (4)$$

It is easily found that $D(r, 0)$ is a Eulerian velocity structure function in space and $D(0, \tau)$ a Lagrangian velocity structure function in time. The Lagrangian velocity structure functions are related to the LVCs by

$$2R(r, \tau) = 2R(0, 0) - D(r, \tau). \quad (5)$$

We present r_c as the intersecting point of the contour $R(r, \tau) = C$ with the space separation axis and τ_c as the intersecting one of the contours $R(r, \tau) = C$ with the time separation axis. The parameter C is a contour level, such that

$$R(r_c, 0) = R(0, \tau_c) = C, \quad (6)$$

which defines the aspect ratio r_c/τ_c . Noting Eq. (5), Eq. (6) implies

$$D(r_c, 0) = D(0, \tau_c). \quad (7)$$

If both r_c and τ_c are within the inertial subrange, we have [19]

$$D(r_c, 0) = C_E(\epsilon r_c)^{2/3}, \quad (8)$$

$$D(0, \tau_c) = C_L(\epsilon \tau_c). \quad (9)$$

Inserting Eqs. (8) and (9) into Eq. (7) gives an expression for the aspect ratios

$$r_c = V\tau_c, \quad (10)$$

where

$$V = (C_L/C_E)^{2/3}(\epsilon\tau_c)^{1/2} \propto \tau_c^{1/2}. \quad (11)$$

Therefore, the aspect ratio satisfies a power law in the inertial range.

We now derive the scale-similarity model: for the crossing point $(0, r_c)$ of the contour with the space separation axis and any other points (τ, r) on the same contour, we have

$$R(r, \tau) = R(r_c, 0). \quad (12)$$

The correlation function $R(r, \tau)$ can be expanded in a Taylor power series about the origin $r=0$ and $\tau=0$ up to a second order [12]

$$\begin{aligned} R(r, \tau) = R(0, 0) &+ \frac{\partial R}{\partial r}(0, 0)r + \frac{\partial R}{\partial \tau}(0, 0)\tau + \frac{1}{2} \frac{\partial^2 R}{\partial r^2}(0, 0)r^2 \\ &+ \frac{\partial^2 R}{\partial r \partial \tau}(0, 0)r\tau + \frac{1}{2} \frac{\partial^2 R}{\partial \tau^2}(0, 0)\tau^2 + O(r^3, r^2\tau, r\tau^2, \tau^3). \end{aligned} \quad (13)$$

The statistically isotropy and stationarity assumptions on the Gaussian velocity fields imply [12]

$$\frac{\partial R}{\partial r}(0, 0) = \frac{\partial R}{\partial \tau}(0, 0) = 0, \quad \frac{\partial^2 R}{\partial r \partial \tau}(0, 0) = 0. \quad (14)$$

Thus, up to a second order approximation, the isocorrelation contours $R(r, \tau)=C$ can be written in the form of

$$r^2 + V^2\tau^2 = C', \quad (15)$$

where

$$V^2 = \frac{\partial^2 R}{\partial \tau^2}(0, 0) \left[\frac{\partial^2 R}{\partial r^2}(0, 0) \right]^{-1}, \quad (16)$$

and C' is a constant. Since both C and C' denote the contour levels, we don't distinguish between them without confusion. Substitution of Eq. (15) into Eq. (12) yields

$$r_c^2 = r^2 + (V\tau)^2. \quad (17)$$

Replacing of r_c in Eq. (12) by Eq. (17) gives the scale-similarity model

$$R(r, \tau) = R(\sqrt{r^2 + V^2\tau^2}, 0). \quad (18)$$

The Taylor series expansion is valid for small separations and thus the model valid only for small separations. To extend this model to larger separations, we need to invoke the scale-similarity assumption of LVCs with a second order approximation to the isocorrelation contours. Under the second-order approximation, we can express the isocorrelation contours by Eq. (15) with an aspect ratio $V=r_c/\tau_c$, that is,

$$r^2 + V^2\tau^2 = C, \quad (19)$$

where the aspect ratio V is implicitly dependent on the separation r_c via the contour level C . The linear terms in Eq. (13) vanishes due to the isotropy and stationarity assumptions on

the Gaussian velocity fields, in which the contours have no any preference direction. In terms of the scale-similarity assumption, the aspect ratio can be determined by Eq. (11). Taking the same procedure as the one from Eq. (15) to Eq. (2), we obtain the scale-similarity model for the separations in the inertial range.

The scale-similarity model suggests that a two-point and two-time LVC can be obtained from an Eulerian velocity correlation and a similarity transformation. The similarity transformation is determined by the isocorrelation contours. It converts between two pairs of space and time separations at which the same correlation value is achieved. The Smith-Hay model is essentially a linear approximation to the isocorrelation contours. It is only valid for "frozen flows." In this case, the particle pairs are convected by the frozen flows which move at a uniform velocity U , without any distortion. The convection velocity was mistaken to determine the Lagrangian decorrelation process. Some corrections to the convection velocity were made to improve the Smith-Hay model with some successes [18]. However, it remains to be a great challenge to determine the convection velocity for the non-frozen flows. The present model proposes a second approximation to the isocorrelation contours. It describes the Lagrangian decorrelation process in the "nonfrozen" flows where the correlation functions decay as either space or time separation increases. The dispersion velocity is defined as the ratio of the spatial length scale to the temporal one. Therefore, it measures the separation velocity of one particle relatively to another fixed particle. The dependence of the dispersion velocity on the equivalent separation r_c confirms that particle dispersions rely on the instantaneous separations. The larger dispersion velocity implies a faster decorrelation process.

To derive the scale-similarity model for LVCs, we assume that the isocorrelation contours have an approximately elliptic shape. This approximation makes it possible to analytically derive the scale-similarity model. The present model is a second approximation to the isocorrelation contours while the Smith-Hay model is a first approximation to the ones. Higher order approximations could be invoked to derive more accurate expressions but they are not necessary for the present purposes. The second order approximation is the least order but most meaningful approximation to the correlation functions.

It is ideal to apply the scale-similarity model to high-Reynolds number turbulence with both space and time separations in the inertial subrange. The inertial subrange becomes infinitely extensive in the limit of infinite Reynolds number. However, in the practical case of finite Reynolds numbers, the inertial subrange is finite [30]. Thus, the space and time separations may belong to the different scaling subranges, such as the dissipation subrange and the inertial subrange. In this case, the scale-similarity model can still survive but the dispersion velocities have to be reformulated. For example, if the temporal separation τ is in the inertial range and the spatial separation r in the dissipation range, we then have Eq. (9) for the temporal separation τ_c and the following equation for the spatial separation r_c :

$$D(r_c, 0) = C_E \frac{\epsilon}{\nu} (r_c)^2. \quad (20)$$

296

297 Using the same procedure as the one from Eq. (7) to Eq.
298 (10), we have

$$V = (C_L/C_E)^{1/2} \left(\frac{\nu}{\tau_c} \right)^{1/2}. \quad (21)$$

299

300 III. DISPERSION VELOCITY IN ISOTROPIC 301 TURBULENCE

302 The dispersion velocity is the only one parameter in the
303 scale-similarity model. In this section, we will analytically
304 calculate the dispersion velocity from the Navier-Stokes
305 equations using the quasinormality assumption. The analyti-
306 cal results obtained will be used to study the Lagrangian
307 decorrelation process.

308 We recall the scale-similarity model of the form

$$309 \quad R(r, \tau) = R(\sqrt{r^2 + V^2 \tau^2}, 0). \quad (22)$$

310 Taking the second-order derivative of both sides of Eq. (22)
311 with respect to τ at $\tau=0$ and $r=r_c$, we obtain

$$312 \quad \frac{\partial^2 R(r_c, 0)}{\partial \tau^2} = \frac{V^2(C)}{r_c} \frac{\partial R(r_c, 0)}{\partial r}. \quad (23)$$

313 The left-hand side of Eq. (23) can be rewritten in Fourier
314 space and further simplified to

$$315 \quad \frac{\partial^2 R(r_c, 0)}{\partial \tau^2} = \int_{-\infty}^{+\infty} \frac{\partial^2 Q(k, 0)}{\partial \tau^2} \exp(-i\mathbf{k} \cdot \mathbf{r}_c) d^3\mathbf{k} \\ 316 \quad = \int_0^{+\infty} \frac{\partial^2 Q(k, 0)}{\partial \tau^2} \frac{\sin(kr_c)}{kr_c} 4\pi k^2 dk, \quad (24)$$

317 where $Q(k, \tau) = \langle \hat{u}_i(\mathbf{k}, t) \hat{u}_i(-\mathbf{k}, t + \tau) \rangle$ is the time correlation of
318 velocity modes $\hat{u}_i(\mathbf{k}, t)$, seeing Eq. (2.26) on page 23 of the
319 classic book on DIA [10]. The time derivative of the mode
320 correlation can be evaluated using the Navier-Stokes equa-
321 tions and the quasinormality assumption, whose details can
322 be found from the derivation of Eq. (16b) in Ref. [31]. In the
323 evaluations, the time derivatives of velocity components in
324 the mode correlations can be calculated from the Navier-
325 Stokes equations, which yield the quadruple correlations. If
326 the velocity fields are quasinormal, the quadruple correla-
327 tions can be expressed by their pair correlations. It is shown
328 [32] that the quasinormality assumption is a reasonable ap-
329 proximation to calculate Eulerian and Lagrangian time cor-
330 relations in isotropic turbulence. This evaluation gives

$$331 \quad \frac{\partial^2 Q(k, 0)}{\partial \tau^2} = -kQ(k, 0) \int_0^{+\infty} qE(q)j(q/k)dq, \quad (25)$$

332 where $E(k) = 2\pi k^2 Q(k, 0)$ is the energy spectra and

$$333 \quad j(x) = \frac{(a^2 - 1)^2 \log \frac{1+a}{1-a} - 2a + \frac{10}{3}a^3}{4a^4},$$

$$a = \frac{2x}{1+x^2}. \quad (26) \quad 334$$

Submitting Eq. (25) into Eq. (24), we obtain 335

$$\frac{\partial^2 R(r_c, 0)}{\partial \tau^2} = -2 \int_0^{+\infty} kE(k)dk \int_0^{+\infty} qE(q)j(q/k) \frac{\sin(kr_c)}{kr_c} dq. \quad (27) \quad 336$$

The integrations in Eq. (27) are symmetric about q and k , 337
and $j(q/k) \approx 16q/15k$ for $q/k < 1$. These considerations lead 338
to 339

$$\frac{\partial^2 R(r_c, 0)}{\partial \tau^2} = -4 \int_0^{+\infty} kE(k) \int_0^k qE(q)j(q/k) \frac{\sin(kr_c)}{kr_c} dq dk \\ = -\frac{64}{15} \int_0^{+\infty} E(k) \frac{\sin(kr_c)}{kr_c} dk \int_0^k q^2 E(q) dq. \quad (28) \quad 340$$

Inserting Eq. (28) into Eq. (23) gives an expression for the 342
dispersion velocity 343

$$V^2 = \frac{64}{15} \int_0^{+\infty} E(k) \frac{\sin(kr_c)}{kr_c} dk \int_0^k q^2 E(q) dq \left[\frac{R(r_c, 0)}{r_c} \right]^{-1}. \quad (29) \quad 344$$

The dispersion velocity V depends on the spatial chord 345
length r_c . The spatial chord length r_c represents the charac- 346
teristic length scale of the isocorrelation contour $R(r, \tau) = C$, 347
while the temporal chord length τ_c represents the character- 348
istic time scale of the isocorrelation contour $R(r, \tau) = C$ such 349
that $R(0, \tau_c) = C$. Therefore, the dispersion velocity is a local 350
quantity. However, the sweeping velocity in Eulerian time 351
correlations is a global one. Note that the sweeping velocity 352
for the two-point and two-time Eulerian velocity correlations 353
is given by [11,16] 354

$$U^2 = \int_0^{+\infty} E(k) dk. \quad (30) \quad 355$$

If the characteristic length scale r_c is very small, for example 356
 $r_c \rightarrow 0$, then $\sin(kr_c)/kr_c \rightarrow 1$ and $R(r_c, 0)/r_c \rightarrow R_r(0, 0)$ 357
 $= \frac{2}{3} \int_0^{+\infty} k^2 E(k) dk$. The dispersion velocity V can be thus sim- 358
plified to 359

$$V^2 = \int_0^{+\infty} E(k) dk \int_0^k q^2 E(q) dq \left[\int_0^{+\infty} k^2 E(k) dk \right]^{-1}. \quad (31) \quad 360$$

Therefore, the dispersion velocity is determined by the en- 361
strophy $\int_0^k q^2 E(q) dq$ in addition to the energy spectra $E(k)$. 362

Comparing Eq. (30) with Eq. (31) gives 363

$$\int_0^{+\infty} k^2 E(k) dk [U^2 - V^2] = \int_0^{+\infty} E(k) dk \int_k^{+\infty} q^2 E(q) dq > 0. \quad (32) \quad 364$$

This implies that the Lagrangian dispersion velocity is 365
smaller than the Eulerian sweeping velocity. Therefore, the 366
LVCs decay more slowly than the Eulerian velocity correla- 367
tions in time. This result is consistent with the one obtained 368

TABLE I. Relevant parameters and statistic quantities in the DNS.

Simulation grid	128 ³	256 ³
Re _λ	66.4	102.05
u'	18.73	18.59
L _f	1.925	1.819
λ	0.4358	0.2675
η	0.0272	0.0135
CFL	0.56	0.3150
k _{max} η	1.158	1.1479

from the LHDIA [23], the dimensional analysis [33] and the Taylor series expansion [31].

An extension of the scale-similarity model to turbulent shear flows is possible. Here, we only present a formal extension to homogeneous sheared turbulence. In this case, the isocorrelation contours remain elliptic in shape. Therefore, the scale-similarity model has the same expression as the one for isotropic turbulence. The dispersion velocity in the model can be formally calculated, which is given by

$$V^2 = \frac{\int_0^{+\infty} \left[\frac{1}{3} S^2 + \frac{32}{15} \int_0^k q^2 E(q) dq \right] \frac{\sin(kr_c)}{kr_c} E(k) dk}{\frac{1}{r_c^2} \int_0^{+\infty} \left[\frac{\sin(kr_c)}{kr_c} - \cos(kr_c) \right] dk}, \quad (33)$$

where S is a shear rate associated with the mean velocity: $U_1 = Sy$, $U_2 = 0$, and $U_3 = 0$. It can be found from Eq. (33) that the shear increases the dispersion velocity and thus enhances the Lagrangian decorrelation process. Further studies are needed to validate the scale-similarity model in turbulent shear flows.

IV. NUMERICAL VERIFICATION OF THE SCALE-SIMILARITY MODEL

The DNS for isotropic turbulence was performed using a pseudospectral method. The computational domain of the three-dimensional Navier-Stokes equations is a box of each side length $L = 2\pi$, where the periodic boundary conditions are applied. To maintain the turbulence stationary, an external force $f(k)$ is imposed on the first two shells of wavenum-

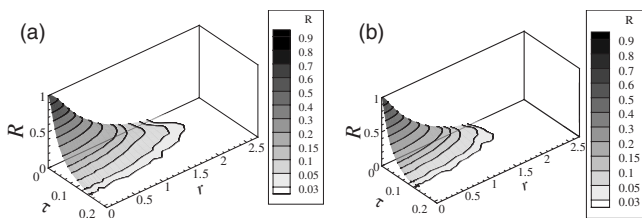


FIG. 1. The surfaces of the Lagrangian velocity correlations as functions of space and time separations at two grids: (a) 128³ and (b) 256³.

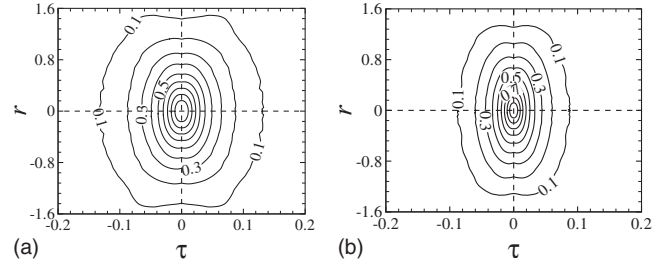


FIG. 2. The isocorrelation contours at two grids: (a) 128³ and (b) 256³.

bers $k=1,2$. Aliasing errors are removed through the two-thirds truncation rule. The Adams-Bashforth scheme is used for time advance. Two cases are run in the present study: case 1 on a 128³ grid and case 2 on a 256³ grid, respectively. The relevant parameters and statistic quantities in the DNS are listed in Table I, where Re_λ is the Taylor-microscale Reynolds number, u' the root-mean-square of velocity fluctuations, L_f the integral length scale, λ the Taylor microscale and η the Kolmogorov length scale. CFL denotes the CFL number. $k_{max}\eta$ describes the spatial resolution.

Figure 1 plots the surface of the Lagrangian velocity correlations obtained from the DNS at two grids 128³ and 256³. The correlation curves decay faster in the direction of time separation axis than the ones in the direction of space separation axis. The surfaces look like paraboloidal in shape.

Figure 2 presents the isocorrelation contours at different levels. They are very different from the straight lines as implied by the Smith-Hay model. They look more like elliptic curves, which supports the assumption on the present scale-similarity model. It is clearly observed that the contours have no any preference direction: their principal axes are coincident with the space and time separation axes respectively. This is different from the Eulerian space-time correlations in turbulent shear flows, where the principal axes are not aligned with either of space and time axes [34,35].

Figure 3 shows the lengths of major axes of the isocorrelation contours as a function of the lengths of their minor axes. The lengths of the axes can be directly calculated from the DNS data: the length of a major axis is the largest distance between two points on the isocorrelation contours and the length of a minor axis is the shortest distance between them. In the present case, the major axis is the space separation one and the minor axis is the time separation one. It can be observed that there exist two scaling subranges: r_c

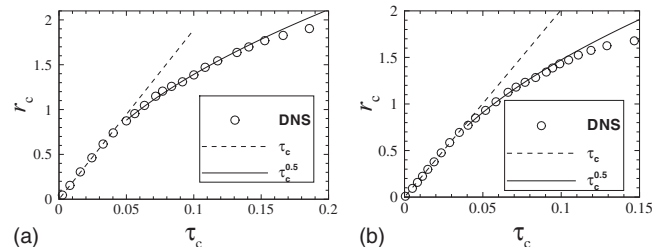


FIG. 3. The lengths of the major axes of the isocorrelation contours as functions of the lengths of the minor axes at two grids: 128³ and (b) 256³.

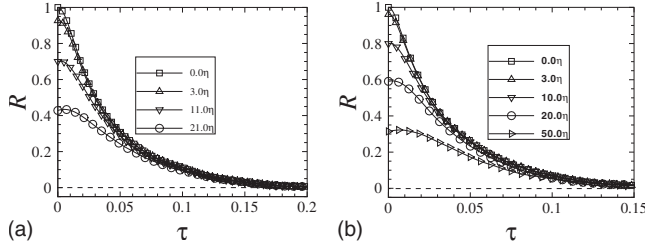


FIG. 4. The Lagrangian velocity correlations for different space separations at two grids: (a) 128^3 and (b) 256^3 .

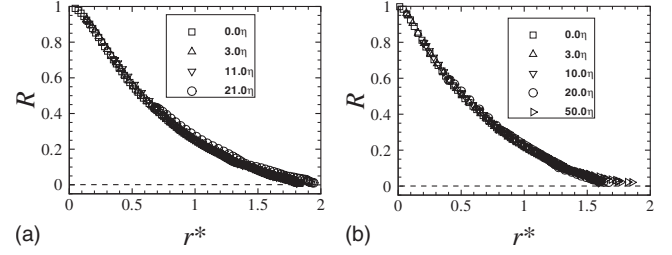


FIG. 5. The Lagrangian velocity correlations for different space separations are plotted against the rescaled separation $r^* = \sqrt{r^2 + (V\tau)^2}$ at two grids: (a) 128^3 and (b) 256^3 .

$\propto \tau_c$ for both r_c and τ_c in the dissipation subrange and r_c
 $\propto \tau_c^{0.5}$ for r_c in the dissipation subrange and τ_c in the inertial
subrange. The scaling ranges for the large Reynolds number
(Re=102.05) are more evident than the one for the small one
(Re=66.40). This observation supports the assumption that
the aspect ratios of the elliptic contours satisfy the scaling
laws.

Figure 4 shows the evolution of the LVCs with time separa-
tion for different initial separations. Those correlation
curves monotonously decrease for initially smaller separa-
tions while they initially increase and then decrease for ini-
tially larger separations. The scale-similarity model predicts
an universal form for the LVCs: $R(r, \tau) = R(\sqrt{r^2 + V^2 \tau^2}, 0)$. If
the LVCs are plotted against the rescaled separations r^*
 $= \sqrt{r^2 + V^2 \tau^2}$, the curves R versus r^* for different separations r
should collapse into the universal form $R(r^*, 0)$. Figure 5
plots those curves together against the rescaled separation
axis defined by $r^* = \sqrt{r^2 + V^2 \tau^2}$. The dispersion velocity V here
is calculated from the DNS data, which is the aspect ratio of
the isocorrelation contours. Evidently, those curves collapse
to a single curve. This collapse supports the scale-similarity
model.

V. DISCUSSION AND CONCLUSIONS

In summary, we develop a scale-similarity model for
LVCs in isotropic turbulence

$$R(r, \tau) = R(\sqrt{r^2 + V^2 \tau^2}, 0), \quad (34)$$

which relates the Lagrangian velocity correlations $R(r, \tau)$ to
the space correlations $R(r, 0)$. The dispersion velocity can be
obtained from the following two equations

$$V^2 = \frac{64}{15} \int_0^\infty \left[E(k) \frac{\sin(kr_c)}{kr_c} \int_0^k q^2 E(q) dq \right] \\ \times dk \left[-\frac{1}{r_c} \frac{\partial R(r_c, 0)}{\partial r} \right]^{-1}, \quad (35)$$

$$r_c^2 = r^2 + V^2 \tau^2. \quad (36)$$

This model suggests an interpretation of the Lagrangian
decorrelation process: a fluid element is distorted by the ed-
dies of the sizes comparable with the fluid element. The dis-
persion velocity measures the particle separations induced by

the distortion of the fluid element. The Lagrangian decorrela-
tion process is very different from the Eulerian decorrela-
tion process, in which small eddies are swept by the energy-
containing eddies and the sweeping velocity dominates this
decorrelation process. An analytical calculation shows that
the dispersion velocity is smaller than the sweeping one.
Therefore, the Lagrangian decorrelation process is more
slowly than the Eulerian decorrelation one.

The scale-similarity model is a second approximation to
the isocontours of Lagrangian velocity correlations, while the
Hay-Smith model is a first approximation to the ones. The
isocorrelation contours offer a transformation between the
Lagrangian and Eulerian velocity correlations. As a conse-
quence of the classic Kolmogorov similarity hypothesis, the
transformation should be scale similar. The DNS of iso-
tropic turbulence supports the scale-similarity model: the
correlation functions exhibit a fair good collapse, when plot-
ted against the normalized space and time separations de-
fined by the model.

The scale-similarity model implies that Lagrangian veloc-
ity correlations are mainly determined by the energy spectra
and the dispersion velocities. Since the dispersion velocities
are mainly determined by enstrophy spectra in addition to the
energy spectra, one can conclude that an accurate prediction
of LES on the energy spectra may not ensure the accurate
prediction of Lagrangian velocity correlations. The typical
class of eddy viscosity SGS models is constructively based
on the energy balance equations. Therefore, it may not cor-
rectly predict the Lagrangian velocity correlations. The criti-
cal comparison between the Lagrangian velocity correlations
in DNS and the ones in LES supports this conclusion [14].
Therefore, the present model may offer a clue to develop the
SGS modeling for LES of particle-laden turbulence.

ACKNOWLEDGMENTS

This work was supported by Chinese Academy of Sci-
ences under the Innovative Project “Multiscale modeling and
simulation in complex systems” (Grant No. KJCX-SW-L08),
National Basic Research Program of China (973 Program)
under Project No. 2007CB814800 and National Natural Sci-
ence Foundation of China under Projects No. 10325211, No.
10628206, No. 10732090, and No. 10702074. G.J. acknowl-
edges the LNM special funding for young investigators.

- 505 [1] L. F. Richardson, Proc. R. Soc. London, Ser. A **110**, 709
506 (1926). 531
- 507 [2] B. L. Sawford, Annu. Rev. Fluid Mech. **33**, 289 (2001). 532
- 508 [3] P. K. Yeung, Annu. Rev. Fluid Mech. **34**, 115 (2002). 533
- 509 [4] G. I. Taylor, Proc. London Math. Soc. **s2-20**, 196 (1922). 534
- 510 [5] G. K. Batchelor, Q. J. R. Meteorol. Soc. **76**, 133 (1950). 535
- 511 [6] G. K. Batchelor, Proc. Cambridge Philos. Soc. **48**, 345 (1952). 536
- 512 [7] L. I. Zaichik and V. M. Alipchenkov, Phys. Fluids **15**, 1776
513 (2003). 537
- 514 [8] G.-W. He and Z.-F. Zhang, Phys. Rev. E **70**, 036309 (2004). 538
- 515 [9] M. W. Reeks, J. Fluid Mech. **522**, 263 (2005). 539
- 516 [10] D. C. Leslie, *Modern Development in the Theory of Turbu-*
517 *lence* (Oxford University Press, London, 1972). 540
- 518 [11] R. H. Kraichnan, Phys. Fluids **7**, 1723 (1964). 541
- 519 [12] T. Gotoh, R. S. Rogallo, J. R. Herring, and R. H. Kraichnan,
520 Phys. Fluids A **5**, 2846 (1993). 542
- 521 [13] R. Rubinstein and Y. Zhou, Phys. Fluids **11**, 2288 (1999). 543
- 522 [14] Y. Yang, G.-W. He, and L.-P. Wang, J. Turbul. **9**, 1 (2008). 544
- 523 [15] G.-W. He, R. Rubinstein, and L.-P. Wang, Phys. Fluids **14**,
524 2186 (2002). 545
- 525 [16] G.-W. He, M. Wang, and S.-K. Lele, Phys. Fluids **16**, 3859
526 (2004). 546
- 527 [17] F. B. Smith and J. S. Hay, Q. J. R. Meteorol. Soc. **87**, 82
528 (1961). 547
- 529 [18] B. L. Sawford, Q. J. R. Meteorol. Soc. **108**, 191 (1982). 548
- 530 [19] A. S. Monin and A. M. Yaglom, *Statistical Fluid Mechanics*,
531 edited by J. Lumley (MIT Press, Cambridge, MA, 1975), Vols. **531**
1 and 2. 532
- [20] R. H. Kraichnan, Phys. Fluids **9**, 1728 (1966). 533
- [21] S. Corrsin, *Proceeding of the Oxford Symposium on Atmo-*
534 *spheric Diffusion and Air Pollution* (Academic, New York, **535**
1960), p. 162. 536
- [22] R. H. Kraichnan, J. Fluid Mech. **81**, 385 (1977). 537
- [23] R. H. Kraichnan, Phys. Fluids **8**, 575 (1965). 538
- [24] Y. Kaneda, Fluid Dyn. Res. **39**, 526 (2007). 539
- [25] T. Gotoh and Y. Kaneda, Phys. Fluids A **3**, 2426 (1991). 540
- [26] P. A. Durbin, J. Fluid Mech. **100**, 279 (1980). 541
- [27] M. S. Borgas and B. L. Sawford, J. Fluid Mech. **279**, 69
542 (1994). 543
- [28] D. J. Thomson, Atmos. Environ. **25A**, 1725 (1991). 544
- [29] M. Bourgoïn, N. T. Ouellette, H. T. Xu, J. Berg, and E. Boden-
545 schatz, Science **311**, 835 (2006). 546
- [30] G.-W. He, S.-Y. Chen, R. H. Kraichnan, R. Zhang, and Y.
547 Zhou, Phys. Rev. Lett. **81**, 4636 (1998). 548
- [31] Y. Kaneda, Phys. Fluids A **5**, 2835 (1993). 549
- [32] Y. Kaneda, T. Ishihara, and G. Koji, Phys. Fluids **11**, 2154
550 (1999). 551
- [33] H. Tennekes, J. Fluid Mech. **67**, 561 (1975). 552
- [34] G.-W. He and J.-B. Zhang, Phys. Rev. E **73**, 055303(R)
553 (2006). 554
- [35] X. Zhao and G.-W. He, Phys. Rev. E **79**, 046316 (2009). 555